Modeling the Mass Transfer in Solvent-Extraction Processes with Hollow-Fiber Membranes

S. Bocquet, A. Torres, J. Sanchez, and G. M. Rios
Institut Européen des Membranes-UM2, 34095 Montpellier Cedex 5, France

J. Romero
Depto. Ingeniería de Química, Universidad de Santiago de Chile, Santiago, Chile

DOI 10.1002/aic.10461
Published online February 28, 2005 in Wiley InterScience (www.interscience.wiley.com).

This work focuses on the modeling of solvent-extraction processes carried out in a hollow-fiber membrane contactor (HFC). A resistance-in-series model has been adapted to deal with a conventional solvent or a nonconventional solvent in subcritical conditions. Two kinds of applications have been chosen to test its validity: extraction of ethanol or acetone from an aqueous solution by subcritical carbon dioxide or propane in a single-fiber module, and extraction of sulfur aroma compounds by hexane. Modifications in membrane characteristics and operating parameters have been investigated to determine optimal conditions. Simulations carried out with carbon dioxide have shown that the resistance in the solvent boundary layer is always negligible, whereas, in the case of hexane, the resistance in the aqueous boundary layer is always predominant. For the application with subcritical carbon dioxide, optimal values of feed and solvent velocities have been obtained. These thresholds correspond to the point where the resistance in the membrane becomes predominant. © 2005 American Institute of Chemical Engineers *AIChE J,* 51: 1067–1079, 2005
Keywords: membrane contactor, modeling, simulation, solvent extraction, subcritical, mass transfer

Introduction

Recently, new processes using membranes as separation devices, the so-called *membrane contactors*, have been a subject of great interest. In these processes, the membrane acts primarily as a physical barrier between two phases without a significant effect in terms of selectivity. Despite this interest, only very few data are available concerning the mechanisms of mass transfer and the prediction of achievable performance. We recently reported the development of a series resistance model to calculate the aroma transfer in osmotic evaporation process where two liquid phases are separated by a gas layer.[1]

In the present work, we use a similar approach to model another process using a membrane device where two nonmiscible liquids are in contact. In this case the solutes are extracted from an aqueous solution by using a membrane-based solvent extraction with a conventional (hexane) and a subcritical solvent (carbon dioxide or propane). A membrane-assisted solvent-extraction process is very attractive compared to classical processes such as dispersion column or mixer–settler. Among a number of advantages, we can point out a perfectly controlled and relatively high interfacial area, no flooding, and no loading so that the flow rate of each phase can be chosen independently. In addition we do not need liquids with different densities because the phases are separated by the membrane and, consequently, emulsions cannot be formed. Nevertheless, the presence of the membrane is also responsible for some drawbacks: it introduces a new resistance to mass transfer; fouling

Correspondence concerning this article should be addressed to J. Sanchez at jose.sanchez@iemm.univ-montp2.fr.

can occur; the membrane has a limited life, so that the cost of the replacement has to be taken into consideration; finally, the membrane contactors could be subject to shell side bypassing.

In this work, we focus on hollow-fiber membrane contactors (HFCs). The aqueous solution containing the solute flows inside the fibers, whereas the solvent flows on the shell side. Because we use a hydrophobic microporous membrane, the solvent will wet the pores and the interface will take place at the mouth of the pore in the inner side of the fiber. At the interface, the solute can be transferred from the aqueous phase to the solvent.

Membrane-based extraction processes with hollow-fiber contactors are used to separate organic solutes from water: acetic acid and phenol using MIBK (methyl isobutyl ketone) or xylene and succinic acid using *n*-butanol as the extracting phase.[2]

The PoroCrit process[3] is based on the use of a sub- or supercritical solvent instead of a conventional one in an HFC to extract a solute. This process is used to carry out the continuous countercurrent extraction of MTBE (methyl *tert*-butyl ether) with subcritical carbon dioxide, using a polypropylene membrane having a mean pore diameter of 2 μm.

The replacement of the conventional solvent by a sub- or supercritical one allows reduction of the resistance to the transfer on the solvent side because of its specific properties (such as high diffusivity, low density, etc.).

Nowadays, supercritical carbon dioxide is widely used as an extraction solvent because of its low critical values and noninjurious nature. Some published examples concern the purification of used frying oil,[4] extraction of natural pigments such as β-carotene,[5] extraction of zinc(II),[6] or the fractionation of fish oils.[7]

Classically, the separation of the supercritical solvent from the extracted solute is achieved by decompression. This leads to savings of energy or the design of acceptable green processes with carbon dioxide. Recently, Tan and coworkers[8] and Bittencourt and coworkers[9] proposed the extraction of solute by using a membrane process such as nanofiltration or reverse osmosis. The same type of coupled process was also reported by Sarrade et al.[10] for the purification of β-carotene or the fractionation of triglycerides of fish oil.

Instead of considering a two-step process, first the extraction of a liquid or solid solute with supercritical carbon dioxide and then the use of a membrane to separate the solute, this work aims to analyze the integration of the two steps—extraction and separation—in one single operation.

Theoretical Approach

This work aims to model the transfer of an organic solute from an aqueous solution toward a conventional (hexane) or a subcritical solvent (propane or carbon dioxide) in an HFC using a countercurrent configuration.

The feed solution flows inside the fibers and the solvent, in the shell side. Our focus here is on the application of the subcritical solvent because a model concerning the application with hexane was previously described in the literature by Pierre et al.[11] The differences between this previous model and our model concerns the solvent phase and the configuration of the contactor (single fiber vs. fiber lumen). However, the same correlations are applicable in the aqueous boundary layer and in the membrane fiber.

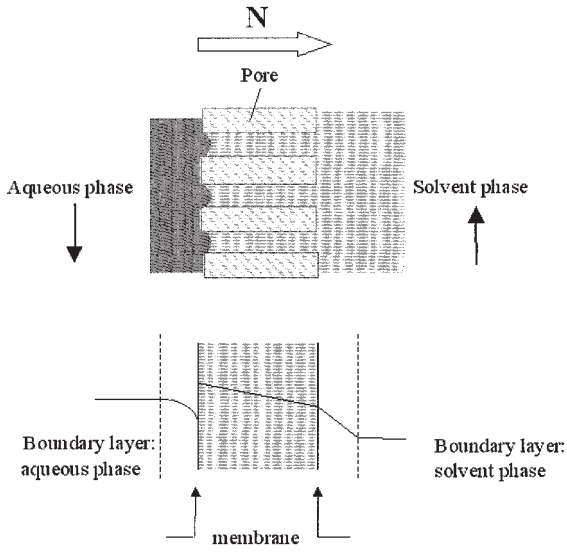

Figure 1. Concentration profiles scheme.

Hypothesis

The model is established with the following assumptions:

- The system works at stationary conditions
- Equilibrium is reached at the fluid–fluid interface
- Each compartment (shell and tubes) is considered to constitute ideally mixed cells
- Laminar flow is fully developed in the contactor
- Pore size and wetting characteristics are uniform along the whole membrane
- The curvature of the interface does not significantly affect mass transfer, solute distribution, or interfacial area
- Mass transfer is correctly described by the boundary layer model
- No transport occurs in the nonporous part of the membrane
- Fluids are immiscible
- The partition coefficient of the solute is constant in the concentration range considered
- Solvent wets the pores and the aqueous–solvent interface settles at the mouth of the pore on the inner side of the membrane
- There is only one solute to be extracted in the feed solution

Resistance-in-series model

The transfer can be described by taking in consideration four steps (Figure 1):

(1) Solute flow through the aqueous boundary layer

(2) Solute crossing the aqueous–solvent interface in the membrane

(3) Solute diffusion in the pore filled with the solvent phase

(4) Solute flow through the solvent boundary layer

The basic idea of the program is that the solute flow is the same at each step of the model and equal to the quantity of

solute gained by the solvent between the inlet and outlet of the extractor.

$$N_w = N_m = N_s = Q_s(C_s^{out} - C_s^0) = N \tag{1}$$

$$N_w = A_{int} k_w \Delta C_w \tag{2}$$

$$N_{mb} = A_{\mathrm{lm}} k_m \Delta C_m \tag{3}$$

$$N_s = A_{ext} k_s \Delta C_s \tag{4}$$

The solute encounters three in-series resistances to the transfer in the aqueous boundary layer, in the membrane, and the last in the solvent boundary layer, respectively.

The resulting resistance to the global transfer is expressed as

$$R = R_{int} + R_m + R_{ext} \tag{5}$$

For a hydrophobic membrane, Gabelman and Hwang[2] give the expression

$$R = \frac{1}{\pi L}\left(\frac{1}{d_{int}k_w} + \frac{1}{P_e d_{\mathrm{lm}} k_m} + \frac{1}{P_e d_{ext} k_s}\right) \tag{6}$$

The corresponding expressions of the overall mass transfer coefficient are:

Shell (or Solvent) Side

$$\frac{1}{K_s} = \frac{P_e}{k_w} + \frac{d_{int}}{d_{\mathrm{lm}} k_m} + \frac{d_{int}}{d_{ext} k_s} \tag{7}$$

Tube (or Aqueous) Side

$$\frac{1}{K_w} = \frac{1}{k_w} + \frac{d_{int}}{d_{\mathrm{lm}} k_m P_e} + \frac{d_{int}}{d_{ext} k_s P_e} \tag{8}$$

Equations

Transport equations

Inside the Fibers. The Levêque relation is usually used to predict the mass transfer coefficient k_w associated with the circulation of a solution inside the fibers[12]:

$$\mathrm{Sh} = 1.62\ \mathrm{Gz}^{1/3} \tag{9}$$

Pierre[13] demonstrates that this equation overestimates the transfer coefficient for the Graetz (Gz) number values < 6. However, his experimental results were better matched using the relations expressed in Eqs. 10 and 11. Therefore, we use

$$\mathrm{Sh} = 0.5\ \mathrm{Gz} \qquad \text{for } \mathrm{Gz} < 6 \tag{10}$$

and

$$\mathrm{Sh} = 1.62\ \mathrm{Gz}^{1/3} \qquad \text{for } \mathrm{Gz} \geq 6 \tag{11}$$

$$N_w = A_{int} k_w (C_{wb} - C_w^i) \tag{12}$$

In the Membrane. Once the solute has crossed the fluid–fluid interface, the transport phenomenon is solely attributable to solute diffusion in the solvent phase.

The value of the transfer coefficient k_m greatly depends on the properties of the membrane (tortuosity, porosity, and thickness) according to Gabelman and Hwang.[2]

For the porosity, the following model[14] has been adopted

$$\tau = \frac{(2 - \varepsilon)^2}{\varepsilon} \tag{13}$$

For $\varepsilon > 5\%$

$$k_m = \frac{\varepsilon}{\tau}\frac{D_s}{\delta} \tag{14}$$

$$N_m = A_m k_m (C_s^i - C_{sm}) \tag{15}$$

On the Shell Side. One of our most troublesome points was to find an appropriate correlation to describe the flow of the subcritical solvent on the shell side. Only a few correlations are available today, among which we can distinguish the following:

(1) Wakao and Kaquei[15]

$$\mathrm{Sh} = 2 + 1.1\ \mathrm{Sc}^{1/3}\mathrm{Re}^{0.6} \tag{16}$$

(2) Tan et al.[16]

$$\mathrm{Sh} = 0.38\ \mathrm{Sc}^{1/3}\ \mathrm{Re}^{0.83} \tag{17}$$

(3) Puiggene et al.[17]

$$\mathrm{Sh} = 0.206\ \mathrm{Sc}^{1/3}\ \mathrm{Re}^{0.8} \tag{18}$$

Because from preliminary tests it appeared that these correlations gave similar results, it was decided to use the Wakao–Kaquei correlation for all further simulations.

$$N_s = A_{ext} k_s (C_{sm} - C_{sb}) \tag{19}$$

With the conventional solvent (hexane) the correlation given by Pierre et al.[11] has been used

$$\mathrm{Sh} = 0.8\ \mathrm{Re}^{0.47}\mathrm{Sc}^{0.33} \tag{20}$$

Table 1. Values of Partition Coefficient P_e Used in the Model*

System	DMDS	MTB	DMTS	Acetone	Ethanol
Hexane–Water	92.2	120.6	564.8		
CO_2–Water				3.01	3.15×10^{-2}
Propane–Water				0.35	1.38×10^{-2}

*DMDS, dimethyldisulfide; DMTS, dimethyltrisulfide; MTB, *S*-methyl butanoate.

Table 2. Values of Diffusion Coefficients ($m^2 s^{-1}$) of the Different Solutes at the Considered Conditions

Solute	DMDS*	MTB*	DMTS*	Acetone	Ethanol
Water	44.4×10^{-10}	34.9×10^{-10}	39.4×10^{-10}	12.8×10^{-10}	12.5×10^{-10}
Hexane	10.9×10^{-10}	8.6×10^{-10}	9.7×10^{-10}		
Carbon dioxide				7.3×10^{-8}	7.3×10^{-8}
Propane				1.1×10^{-8}	1.2×10^{-8}

*Data from Pierre et al.[11]

Thermodynamics and fluid properties

Fluid–Fluid Equilibrium. The partition coefficients values of ethanol and acetone between water and carbon dioxide are those indicated by Bothun et al.[18]. They were calculated with a group contribution method given by Gros et al.[19,20]

Likewise, the equilibrium data for sulfur aroma compounds between hexane and water were obtained from the experimental work of Pierre et al.[11] The values for both cases are given in Table 1.

We notice that in the case of sulfur aroma compounds, the partition coefficients are greatly favorable to the solvent phase, which means that the solutes have a much greater affinity for the solvent than for the aqueous phase. In that case we can consider that the transfer in the aqueous boundary layer could control the transfer. In contrast, the values of these coefficients for ethanol and acetone in propane and carbon dioxide in subcritical conditions are quite small (<1), except for acetone in carbon dioxide (3.01). Thus, it is difficult at this point to predict which step will limit the mass transfer during the extraction with the subcritical solvent.

Diffusion Coefficient. The diffusion coefficients in water were calculated with the Wilke–Chang correlation,[21] whereas those in carbon dioxide were determined with the Catchpole–King correlation,[22] the values of which are reported in Table 2.

Numerical Methods. The program was written in Matlab® 6.5 (The MathWorks, Natick, MA), which simultaneously determines the solute concentration at the membrane interface on the aqueous side, the concentration at the water–solvent interface on the solvent side, the concentration at the outlet of the pore, and the bulk concentration in the solvent phase by solving a linear system. The resolution is done using a Matlab function without iterative calculations. The simulation could be carried out changing the operating conditions and the structural parameters of the membrane.

Table 3. Hollow-Fiber Contactor Characteristics and Operating Conditions for Extraction of Sulfur Aroma Compounds with Hexane*

Characteristic/Condition	Type/Value
Type of fibers	Polypropylene
Type of potting	Polyethylene
Porosity	0.25
Tortuosity	2
Pore diameter, μm	30
Number of fibers	10,000
Length of fibers, mm	146
Fiber inside diameter, μm	200
Fiber outside diameter, μm	300
Inside diameter of the hollow-fiber bundle, mm	12
Outside diameter of the hollow-fiber bundle, mm	49
Shell side geometric void fraction	0.40
Temperature, K	298
Pressure	1 atm
Solvent flow rate, mL/s	8.5
Aqueous-phase velocity, m/s	0.15
Recycled streams	Yes

*Data from Pierre et al.[11]

Results and Discussion

Each simulation run furnishes the flux of solute across the membrane (N). The ratio of the quantity of solute transferred to the quantity of solute in the feed solution is also determined. It is hereafter designated the "extraction efficiency" (Eff). Finally, the local and overall mass transfer coefficients; the three resistances R_{int}, R_{mb}, and R_{ext}; and the height of transfer unit based on solvent or aqueous side (HTU_s and HTU_w, respectively) are calculated

$$\text{Eff} = \frac{N}{Q_w C_w^0} \tag{21}$$

$$\text{HTU}_s = \frac{\nu_s}{K_s a} \tag{22}$$

$$\text{HTU}_w = \frac{\nu_w}{K_w a} \tag{23}$$

Model validation

To validate the model we compared our simulation results with those experimentally obtained or simulated in previous publications.[11,18]

Concerning the conventional extraction, we modeled the extraction of three sulfur aroma compounds (DMDS, dimethyldisulfide; DMTS, dimethyltrisulfide; MTB, *S*-methyl butanoate) contained in aqueous solutions at two initial concentrations, 5 and 20 ppm, by hexane.

The operating parameters are listed in Table 3 and results in Table 4.

We can observe that our simulations for the 5 ppm solutions are in good agreement with experimental results: the relative deviations between experimental and simulated values of trans-

Table 4. Validation of Model for Hexane Extraction

Solute	Initial Concentration (ppm)	N (10^7 mol/s)	N_{exp} (10^7 mol/s)*
DMDS	5	12.1	12.0
	20	51.9	77.4–108
DMTS	5	9.19	10.5
	20	37.1	57.7–80.2
MTB	5	8.43	9.90
	20	35.5	61.6–85.7

*Data from Pierre et al.[11]

Table 5. Hollow-Fiber Contactor Characteristics and Operating Conditions for Subcritical Extraction of Ethanol or Acetone*

Characteristic/Condition	Type/Value
Type of fibers	Polypropylene
Porosity	0.75
Tortuosity	2 (Calculated)
Pore diameter, μm	0.4
Number of fibers	1
Length of fibers, mm	1067
Fiber inside diameter, mm	0.6
Fiber outside diameter, mm	1.02
Inside diameter of the hollow-fiber bundle, mm	1.52
Outside diameter of the hollow-fiber bundle, mm	3.18
Temperature, K	298
Pressure	69 bar (CO_2) 34.5 bar (propane)
Initial concentration of the solute in the feed phase, wt %	10
Molar solvent to feed ratio range	1–10
Aqueous flow rate range, mL/min	0.1–2
Recycled streams	No

*Data from Bothun et al.[18]

ferred fluxes are, respectively, 0.8% for DMDS, 12% for DMTS, and 15% for MTB. The results with 20 ppm are less precise, the calculated values of which are always from 30 to 60% lower than the experimental values. It is useful to recall here that the repeatability of the experimental results reported by Pierre et al.[11,23] for the three solutes is not very high. Furthermore, hydrodynamics is certainly much more complex than what our correlation can take into account. In addition, the fibers may be subject to deformation, which can lead to additional errors between experimental and calculated values.

Concerning the subcritical solvent extraction, we studied the extraction of ethanol or acetone in a 10 wt % aqueous solution by propane or carbon dioxide.

The operating parameters are listed in Table 5, whereas the comparison between experimental extraction efficiency, simulated values given in the literature, and simulations carried out in this work are shown in Figures 2–4 and in Tables A1–A4 in the Appendix. Broadly, we can observe that the results here obtained by simulation are in the same order of magnitude order as those already reported.[18] At a constant value of solvent to feed ratio, increasing the velocity of the feed leads to a decrease of efficiency. The limiting step to the transfer is in the aqueous boundary layer. When the velocity of the feed increases, the residence time of the solute diminishes, thus leading to a decrease of Eff. It must be noted that our simulations approach to a greater degree the experimental results in the case of acetone extraction with propane. However, whatever the case, the simulations, although showing good tendencies, overestimate Eff values.

To replace the analysis within an adapted framework, it is advisable to observe that experimental results themselves are not always easy to account for.[18] For example, in the case of extraction of ethanol by propane, for a set molar feed to solvent ratio, there is no clear trend in the variation of the experimental extraction efficiency with increasing feed flow rate, eloquently bearing testimony to variability.

In a second publication, Bothun et al.[24] gives complementary values of HTU_s. For example, their operating parameters were a solvent to feed molar ratio of 1 and a 10% ethanol feed solution in countercurrent with subcritical propane. They found HTU_s values ranging from 0.06 to 0.03 m for a feed flow rate of 0.15 to 2 mL min^{-1}. In this work we found, under the same conditions, HTU_s values ranging from 0.08 to 0.90 m. Under the same operating conditions with a 10% acetone feed solution, the values of HTU_s reported by Bothun et al.[24] vary from 0.19 to 0.4 m, whereas in our case they range from 0.32 to

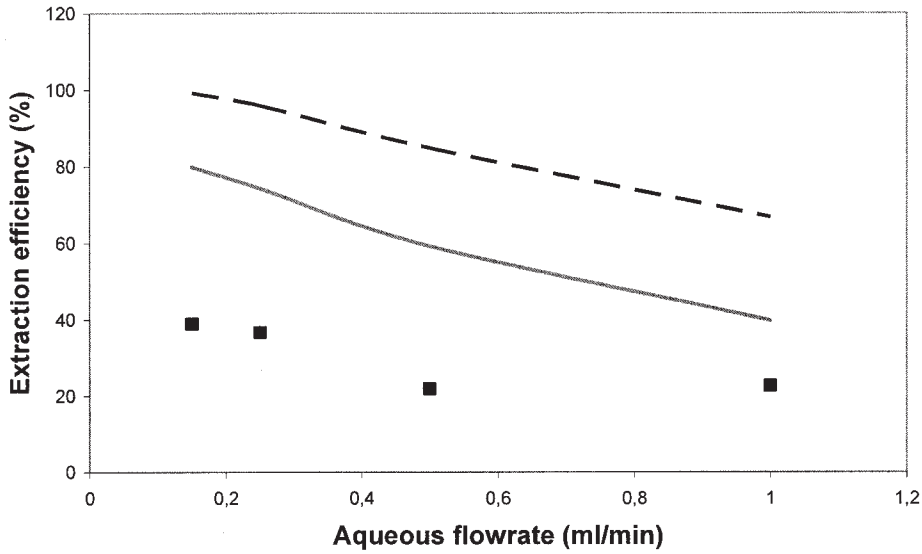

Figure 2. Comparison between experimental extraction efficiency[a] (—■—) and calculated values [in the literature[a] (dashed line) and our simulations (solid line)] in the case of acetone extraction by subcritical propane, for a molar solvent to feed ratio of 1.

[a] Data from Botun et al.[18]

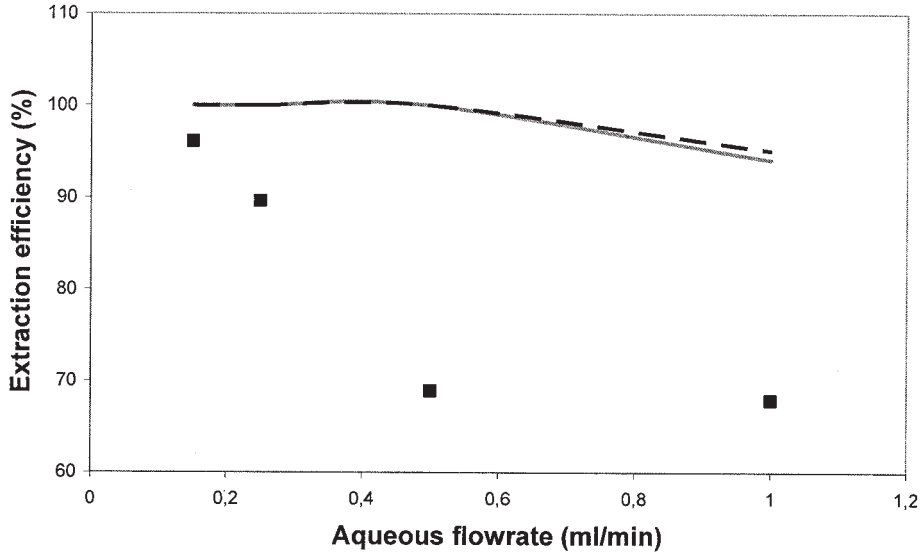

Figure 3. Comparison between experimental extraction efficiency[a] (—■—) and calculated values [in the literature[a] (dashed line) and our simulations (solid line)] in the case of acetone extraction by subcritical carbon dioxide, for a molar solvent to feed ratio of 3.

[a] Data from Botun et al.[18]

0.94 m (these last values for a feed flow rate of 1 mL min^{-1}). With respect to ethanol extraction with subcritical carbon dioxide, they found HTU_s values between 0.12 and 0.45 m, against 0.07 and 0.23 m in this work. The differences thus observed must arise to some extent from the choice of different correlations to calculate the local transfer coefficient in the subcritical solvent phase. Indeed Bothun and coworkers[24] selected—in analogy with liquid–liquid extraction[25] and gas absorption[26]—the following equations

$$\mathrm{Sh} = 1.25\ \mathrm{Sc}^{1/3}\left(\mathrm{Re}\,\frac{d_h}{L}\right)^{0.93} \tag{24}$$

$$\mathrm{Sh} = 5.8\ \mathrm{Sc}^{1/3}\ \mathrm{Re}^{0.6}\,\frac{d_h}{L} \tag{25}$$

In addition, the geometrical characteristics chosen in both publications[18,24] are slightly different: 1.02 mm outer diameter

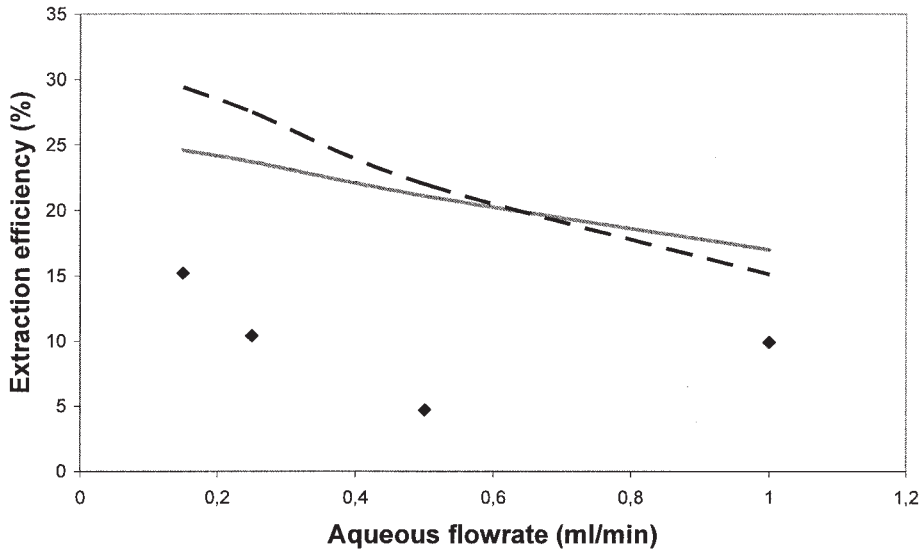

Figure 4. Comparison between experimental extraction efficiency[a] (—■—) and calculated values [in the literature[a] (dashed line) and our simulations (solid line)] in the case of ethanol extraction by subcritical carbon dioxide, for a molar solvent to feed ratio of 3.

[a] Data from Botun et al.[18]

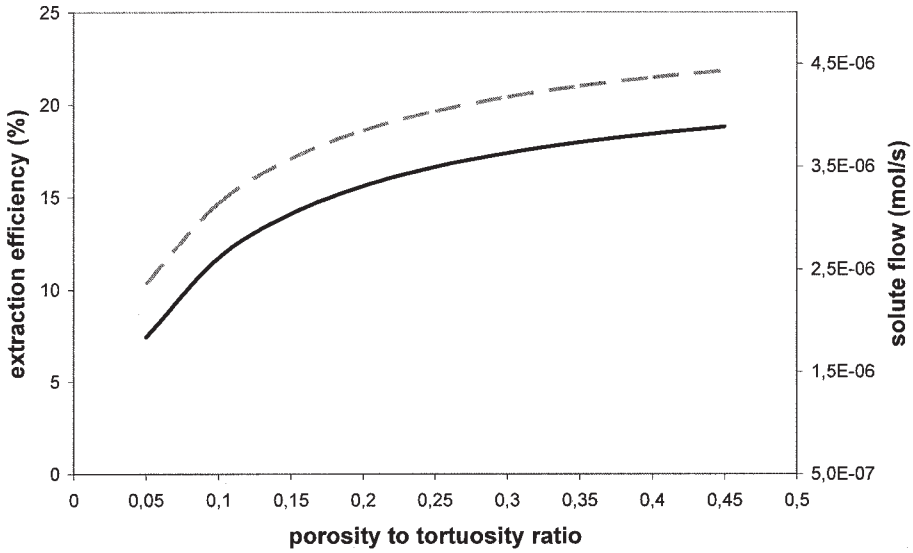

Figure 5. Influence of the porosity to tortuosity ratio on extraction efficiency (dashed line) and transferred solute flux (solid line) in the case of ethanol extraction by subcritical carbon dioxide.

of the fiber and 1.52 mm inner diameter of the steel tube vs. 1 and 1.8 mm, respectively, which presupposes strong differences in solvent hydrodynamics.

The fact is that these experiments are very difficult to put into practice because of high pressure conditions in the module. We can note that those high-pressure conditions (69 bar for carbon dioxide and 34.5 bar for propane) could involve fiber deformation, preferential ways of flux, or some modification of the membrane structure. In that case, the model for hydrodynamic conditions in the fiber or in the shell side can be somewhat far from reality. In spite of these previous considerations, this model can offer a first approach of the phenomenon and can allow simulation of the changes in structure or process parameters.

From this point on, tendencies that emerge when variation of the systems parameters is imposed have been studied. Works have been more particularly focused on two systems: aqueous solution containing 5 ppm DMDS with a velocity of 0.15 m s^{-1} and hexane flowing at 8.5×10^{-6} m^3 s^{-1}; 10% weight ethanol aqueous solution with a volume flow rate of 0.5 mL min^{-1}; and subcritical carbon dioxide with a solvent to feed molar ratio of 3.

Influence of membrane structural parameters

Porosity to Tortuosity Ratio. For simulation purposes we consider a variation of porosity to tortuosity ratio between 0.05 and 0.45 for both applications. These values correspond to classical porous membranes with porosity between 0.2 and 0.9 and tortuosity between 2 and 3 (values given by Gabelman and Hwang[2]). In the case of subcritical extraction with carbon dioxide, we notice that the solute flux and the extraction efficiency are more than doubled, as shown in Figure 5. This parameter does not affect the resistances in the boundary layers but results in a decrease of 90% of the membrane resistance. The global resistance is reduced by 80%.

For all tested values of this ratio, the predominant resistance is the diffusion through the membrane (see Figure 6). Figure 6 represents the relative and cumulative contribution of each step to the global resistance; the value of each single resistance can be read between two curves, as depicted in the figure, which means that the membrane resistance decreases with the porosity/tortuosity ratio enhancement. At a ratio of 0.45 both resistances, in the membrane and in the aqueous boundary layer, are dominant. The resistance in the solvent boundary layer is always negligible (<1%). When the value of the ratio increases, the diffusion in the membrane becomes enhanced, whereas the transfer resistance in the aqueous boundary layer remains unchanged, so the relative contribution of this step becomes increasingly important. We should also remember that the partition coefficient of ethanol between water and subcritical carbon dioxide is much more favorable to water, which can explain why the resistance in the membrane filled with the solvent can be predominant in some cases.

When the resistance in the membrane is predominant, the flux of solute and the extraction efficiency increase very quickly (see Figure 5).

If we now consider the extraction with hexane, we observe a very small increase, about 5%, of the solute and of the extraction efficiency. The global resistance decreases slightly (10%). This parameter scarcely affects the separation because the resistance in the aqueous boundary layer is always predominant (between 94.5 and 99%). This is certainly attributed to the high value of the partition coefficient between hexane and water: the solute has a much higher affinity for the solvent than for water, so that the diffusion step in the membrane filled with the solvent is negligible with respect to the transport in the aqueous boundary layer.

Inner Diameter of the Fibers. We made simulations of the response of Eff when varying the inner diameter of the fibers. To maintain a constant membrane thickness, the inner and outer diameters of the fibers were varied simultaneously. It is important to note that in this case the variation of the fiber diameter also resulted in a modification of the linear velocity or

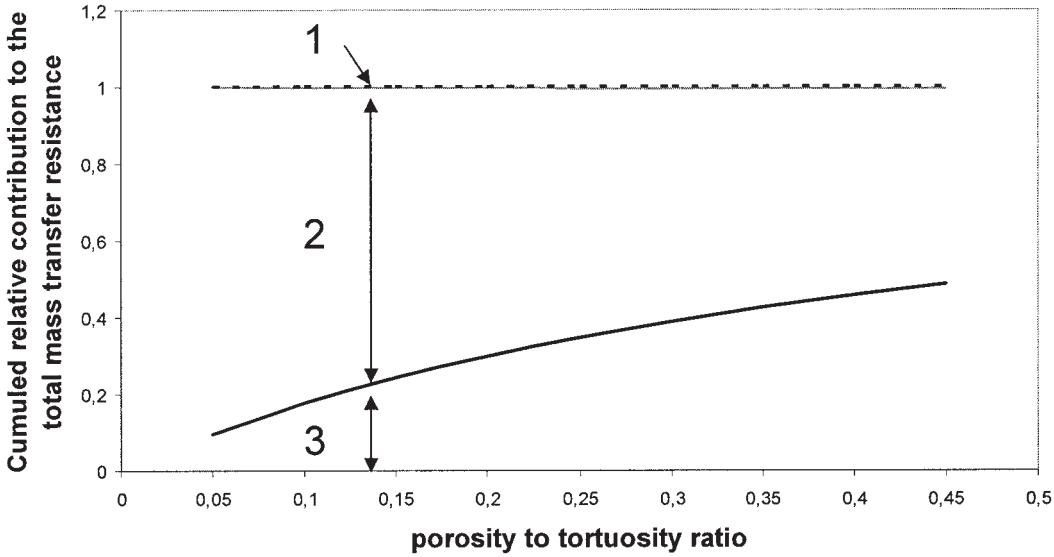

Figure 6. Influence of the porosity to tortuosity ratio on the relative contributions of the local resistances to the overall transfer resistance in the case of ethanol extraction by subcritical carbon dioxide.

1: contribution of the solvent boundary layer resistance; 2: contribution of the membrane resistance; 3: contribution of the aqueous boundary layer resistance.

the flow rate of the aqueous and solvent phases. The simulation curves are shown in Figures 7 and 8.

For the application with subcritical solvent (Figure 7), the range of diameters for the fiber was increased from 0.1 to 0.8 mm. In this case the flow rate was maintained constant and, in consequence, the linear velocity decreases. Indeed, the flux of ethanol and extraction efficiency increased by 40%. With a fiber diameter of 0.1 mm, the predominant resistance is in the membrane (84.8 vs. 15% for the aqueous boundary layer), but when it reaches 0.8 mm, the aqueous boundary layer and membrane represent 62.3 and 36.9% of the total resistance, respectively. When the diameter of the fiber increases, the velocity rate of the aqueous solution decreases. In this case the mass transfer is enhanced because the residence time of the aqueous solution in the extractor is higher. Indeed, the solute has enough time to reach the interface and be transferred to the solvent. The calculation of the overall resistance results in a decrease of 75% of its initial value. As usual, the resistance in the solvent phase is negligible.

With respect to the extraction with hexane, the diameter of the fibers ranges from 0.15 to 0.29 mm. In this case the calculations were made considering a constant linear velocity and, consequently, the flow rate increases and the residence time decreases. Moreover, an increase in the inner diameter of the fibers also results in an increase in transfer surface. Consideration of Eq. 21 shows that the variation of both parameters

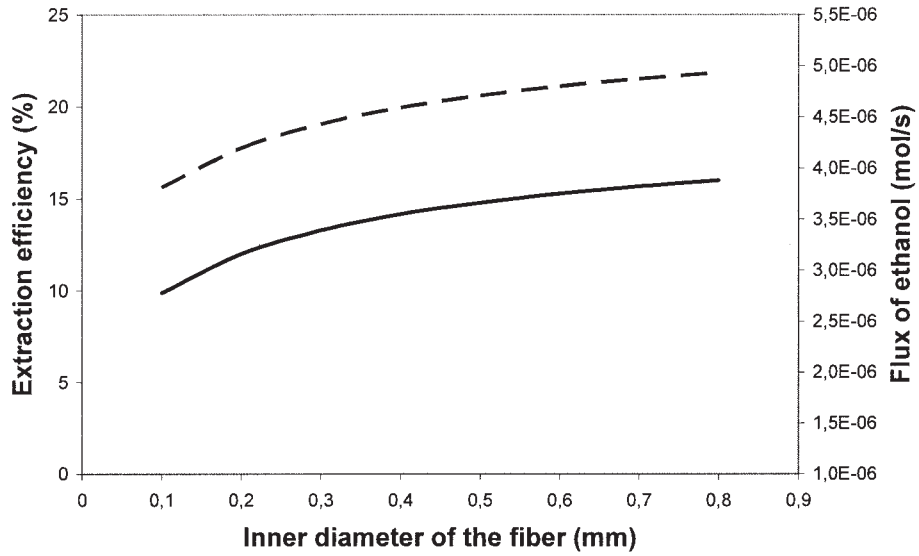

Figure 7. Influence of the inner diameter of the fiber on the transferred flux of ethanol (solid line) and extraction efficiency (dashed line) in the case of ethanol extraction by subcritical carbon dioxide.

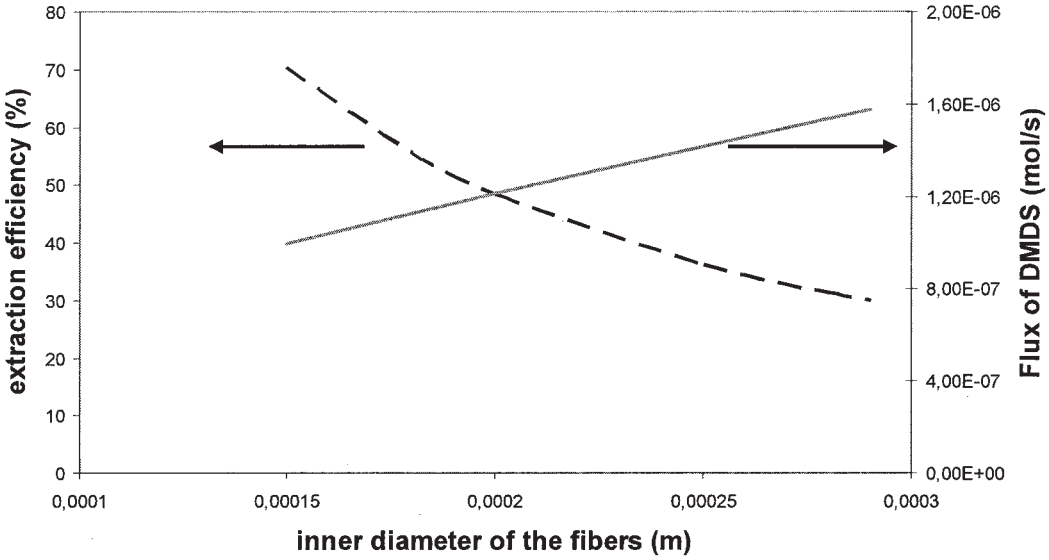

Figure 8. Influence of the inner diameter of the fibers on the transferred flux of DMDS (solid line) and extraction efficiency (dashed line) in the case of DMDS extraction with hexane.

results in an increase of 50% of the DMDS flow, whereas the efficiency decreases. As discussed in the last paragraph, the predominant resistance is always the aqueous boundary layer (between 96.7 and 99.3% of the global resistance).

Influence of process parameters

Velocity of Feed Solution. In this case, we considered two feed solutions, with 5 and 20 ppm of DMDS. The results are shown in Figure 9 for the 5 ppm solution. At constant velocity of the solvent we made simulations increasing the velocity of the feed inside the fibers from 0.06 to 0.2 m s^{-1}. The flux of solute increases to 47% with the velocity of the feed, for a flow rate of hexane of 60 mL min^{-1}, but at the same time the efficiency decreases to 55% of its value. The quantity of solute introduced in the extractor increases, whereas the residence time decreases, which leads to an improvement of the transferred flux but a decrease of the efficiency. The aqueous side resistance is always predominant but decreases slightly with increasing linear velocity (97.7 to 96.6%), similar to that of global resistance. For a 20 ppm solution, we obtain the same

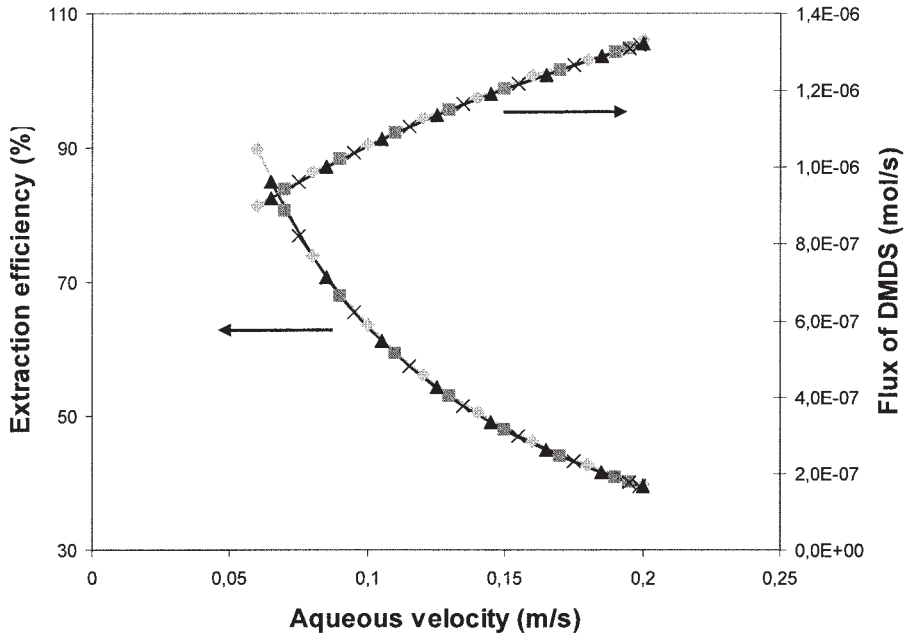

Figure 9. Influence of the velocity of aqueous phase on the extraction efficiency (decreasing curve) and DMDS flux (increasing curve) for different values of hexane flow rate and for a feed solution of 5 ppm DMDS (—■—, 60 mL min^{-1}; —◆—, 510 mL min^{-1}; —▲—, 600 mL min^{-1}; —×—, 3000 mL min^{-1}).

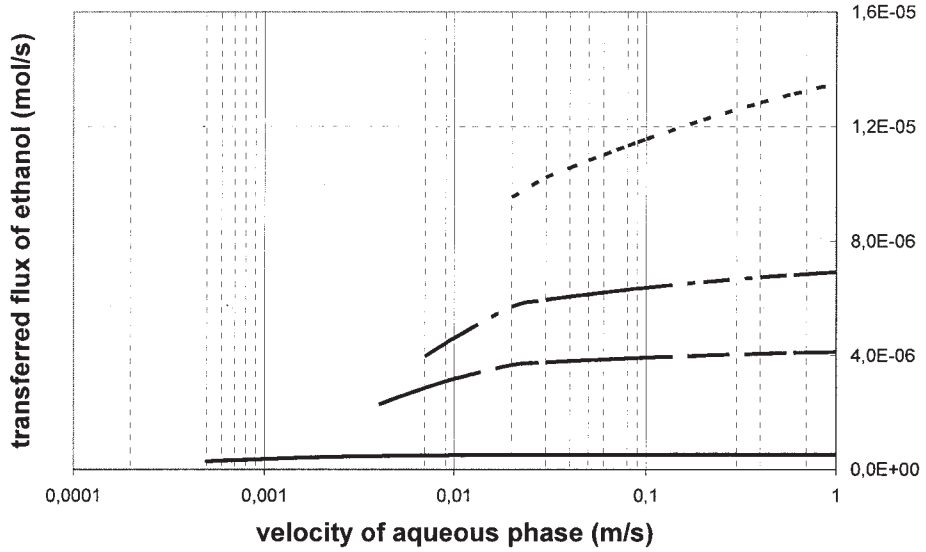

Figure 10. Influence of the velocity of aqueous phase on the transferred flux of ethanol for different values of carbon dioxide velocity (—, 0.00796 m s^{-1}; — – —, 0.0796 m s^{-1}; – – –, 0.167 m s^{-1}; - - -, 0.796 m s^{-1}).

magnitude of variations: 47% of increase of the flux and 55% of decrease for the efficiency (the values of the fluxes being fourfold greater than those for the 5 ppm solution).

For the application with carbon dioxide, we studied the influence of an increase of the feed velocity, where the solvent velocity remained constant. Four values were considered: 0.00796, 0.0796, 0.167, and 0.796 m s^{-1}. As we can observe from Figures 10 and 11, when the feed velocity increases the flux of solute begins to increase until it reaches a threshold, whereas the corresponding extraction efficiency decreases. In Figure 10, for example, for a solvent velocity of 0.0796 m s^{-1} the flux increases quickly to about 60% when the aqueous phase velocity increases from 0.004 to 0.02 m s^{-1} before reaching a nearly constant value. The global increase of the flux is about 75%. At the same time, the efficiency loses 67% of its value (up to 0.02 m s^{-1}) (Figure 11). The calculations of the height of transfer unit HTU_w resulted in an increase from 0.65 to 1.11 m for 0.004 and 0.02 m s^{-1}, respectively. For smaller values of the feed velocity, the resistance in the aqueous boundary layer is predominant (>80% of the global resistance) and then it decreases, whereas the two others remain unchanged. The threshold corresponds to the point where the membrane resistance becomes greater than the resistance in the aqueous side. As it has been observed in previous examples, the resistance in the solvent phase is always negligible. It seems that there is an optimum for the velocity of the feed: if the velocity is too small, the flux is not satisfactory but the efficiency is very high; however, if the velocity is too high, the efficiency is really small and the flux is not proportionally high. The best choice corresponds to the feed velocity reached at the threshold.

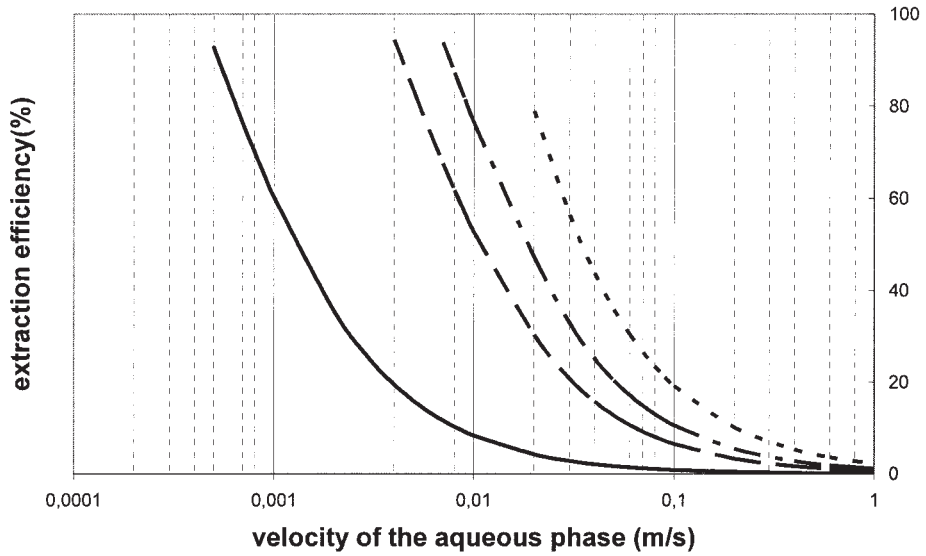

Figure 11. Influence of the velocity of aqueous phase on the extraction efficiency for different values of carbon dioxide velocity (—, 0.00796 m s^{-1}; — – —, 0.0796 m s^{-1}; – – –, 0.167 m s^{-1}; - - -, 0.796 m s^{-1}).

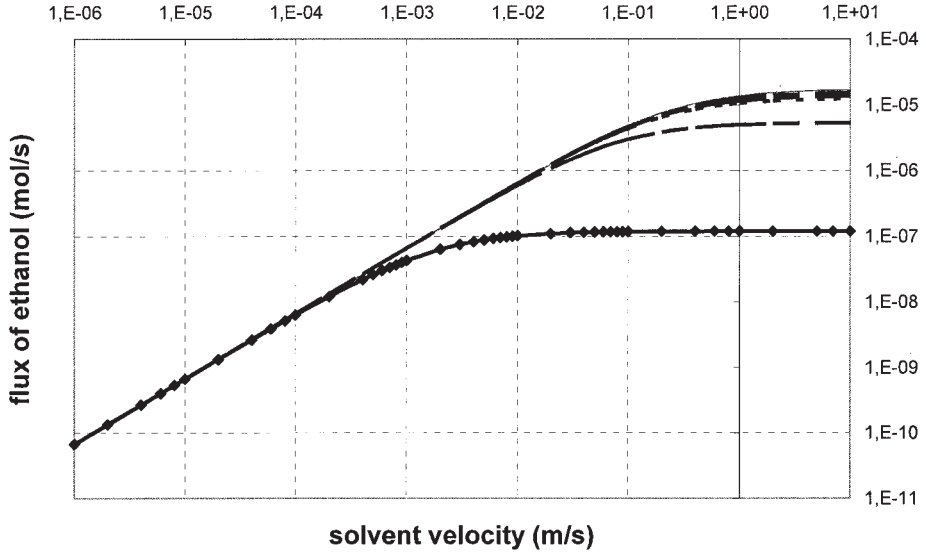

Figure 12. Influence of solvent velocity on the flux of ethanol for different values of the feed velocity (—◆—, 0.0001 m s^{-1}; – – –, 0.00589 m s^{-1}; - - -, 0.0589 m s^{-1}; - - -, 0.0295 m s^{-1}; — – —, 0.167 m s^{-1}; —, 0.589 m s^{-1}).

Velocity of Solvent. In the case of extraction with hexane, four different solvent velocities were considered with the same feed solutions: 5 and 20 ppm of DMDS. From Figure 9 it is obvious that the solvent velocity has no influence on the separation; flux and efficiency remain nearly the same at 60, 510, 600, and 3000 mL min^{-1} (0.6 and 0.5% of variation, respectively). This result could be expected because of the predominant resistance on the aqueous side. Increasing the velocity of the solvent has no influence on the global mass transfer.

In the case of extraction with carbon dioxide, the solvent velocity ranges from 10^{-4} to 10 m s^{-1}. Whatever the feed velocity, it can be observed that, when the velocity of the solvent increases, so do the extraction efficiency and the transferred flux. From Figures 12 and 13 it appears that flux and efficiency reach a threshold for higher values of solvent velocity. Nevertheless, the value of the overall mass transfer coefficient K_w remains essentially the same over the range of solvent velocity investigated (11% of increase) as well as the calculated HTU_w (10% of decrease). At a solvent velocity of 0.0001 m s^{-1}, the resistance in the solvent phase represents 10.6% of the global resistance; then, this local resistance becomes negligible, which explains the small variation of the global resistance and mass transfer coefficient.

From these results it follows that there is an optimal solvent velocity. Because of the presence of the final threshold, this velocity does not need to be too high for a very efficient extraction process.

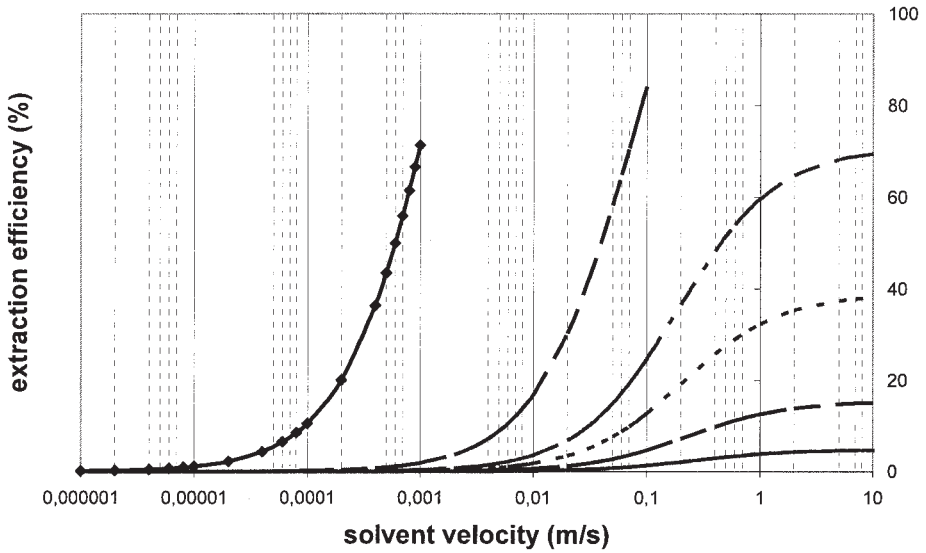

Figure 13. Influence of the solvent velocity on the extraction efficiency for different values of the velocity of feed (—◆—, 0.0001 m s^{-1}; – – –, 0.00589 m s^{-1}; - - -, 0.0589 m s^{-1}; - - -, 0.0295 m s^{-1}; — – —, 0.167 m s^{-1}; —, 0.589 m s^{-1}).

Conclusions

In this work an efficient tool is proposed for the simulation of membrane-based solvent extraction in hollow-fiber contactors. In a first step, it provides useful information to optimize the process. Modifications in the membrane's physical characteristics and process parameters such as fluids velocities have been investigated.

For the application with subcritical solvent, a high porosity to tortuosity ratio is desired for obtaining a high flux and efficiency. The same tendency has been observed for large inner diameter of the fibers and moderate values of solvent and feed velocities. This last result is associated with the presence of a threshold in the flux of solute.

Concerning the second application—that is, the extraction of aroma compounds with hexane—conclusions are somewhat different. Because the predominant resistance to the transfer is always in the aqueous boundary layer, the porosity to tortuosity ratio has no influence on the separation. There is no need to recommend a specific value of this ratio. As before, the inner diameter must be as large as possible. Increasing the feed velocity enhances the flux but causes a decrease in the efficiency; thus, a compromise between these two aspects has to be found. The solvent velocity has no influence on the separation, so that a small value can be chosen with respect to economy.

The enhancement of the model is in progress; in particular, the next version should take into account the axial variation of concentration along the contactor and other variations of the operational parameters of the process. Other correlations for the shell side are currently under investigation.

Notation

a = lumen inner area to volume ratio, m^{-1}
A = interfacial area, m^2
C = concentration, mol m^{-3}
d = diameter, m
D = diffusion coefficient, m^2 s^{-1}
Eff = extraction efficiency
F = feed molar flow rate, mol s^{-1}
Gz = Graetz number
HTU = height of transfer unit, m
k = local mass transfer coefficient, m s^{-1}
K = overall mass transfer coefficient, m s^{-1}
L = length of the fiber, m
N = molar flux, mol s^{-1}
P = pressure, bar
P_e = partition coefficient
Q = volume flow rate, m^3 s^{-1}
R = resistance to the transfer, s m^{-3}
Re = Reynolds number
S = solvent molar flow rate, mol s^{-1}
Sc = Schmidt number
Sh = Sherwood number
T = temperature, K
v = velocity, m s^{-1}

Greek letters

δ = membrane thickness m
ε = porosity
μ = viscosity, Pa·s
ρ = density, kg m^{-3}
τ = tortuosity

Subscripts

b = bulk
cal = relative to the shell
ext = relative to the exterior of the fiber
h = hydraulic
int = relative to the interior of the fiber
lm = logarithmic mean
m = in the membrane
s = solvent side
w = aqueous side

Superscripts

0 = at the inlet of the contactor
Out = at the outlet of the contactor
i = at the aqueous solvent interface

Literature Cited

1. Romero J, Rios GM, Sanchez J, Bocquet S, Saavedra A. Modeling heat and mass transfer in osmotic evaporation process. *AIChE J.* 2003;49:300-308.
2. Gabelman A, Hwang ST. Hollow fiber membrane contactors. *J Membr Sci.* 1999;159:61-106.
3. Sims M. Porocritical fluid extraction from liquids using near-critical fluids. *Membr Technol.* 1998;97:11-12.
4. Yoon J, Han BS, Kang YC, Kim KH, Jung MY, Kwong YA. Purification of used frying oil by supercritical carbon dioxide extraction. *Food Chem.* 2000;71:275-279.
5. Subra P, Castellani S, Jestin P, Aoufi A. Extraction of β-carotene with supercritical fluids. Experiments and modelling. *J Supercrit Fluids.* 1998;12:261-269.
6. Tai CY, You GS, Chen SL. Kinetics study on supercritical fluid extraction of zinc(II) ion from aqueous solutions. *J Supercrit Fluids.* 2000;18:201-212.
7. Catchpole OJ, Grey JB, Noermark KA. Fractionation of fish oils using supercritical CO_2 and CO_2 + ethanol mixtures. *J Supercrit Fluids.* 2000;19:25-37.
8. Tan CS, Lien HC, Lin SR, Cheng HL, Chao KJ. Separation of supercritical carbon dioxide and caffeine with mesoporous silica and microporous silicalite membranes. *J Supercrit Fluids.* 2003;26:55-62.
9. Bittencourt Spricigo C, Bolzan A, Machado RAF, Castelan Carlson LH, Cunha Petrus JC. Separation of nutmeg essential oil and dense CO_2 with a cellulose acetate reverse osmosis membrane. *J Membr Sci.* 2001;188:173-179.
10. Sarrade S, Rios GM, Carlès M. Supercritical CO_2 extraction coupled with nanofiltration separation. Applications to natural products. *Sep Purif Technol.* 1998;14:19-25.
11. Pierre FX, Souchon I, Marin M. Recovery of sulfur aroma compounds using membrane-based solvent extraction. *J Membr Sci.* 2001;187:239-253.
12. Reed BW, Semmens MJ, Cussler EL. Membrane contactors. In: Noble RD, Stern SA, eds. *Membrane Separations Technology. Principles and Applications.* Amsterdam: Elsevier; 1995:467-498.
13. Pierre FX. *Les Contacteurs Membranaires Appliqués à l'Extraction des Composés d'Arômes.* PhD Diss., Institut National Agronomique-Paris Grignou. Dec. 2002. Paris, France.
14. Prasad R, Sirkar KK. Dispersion free solvent extraction with microporous hollow-fiber modules. *AIChE J.* 1988;34:177-188.
15. Skerget M, Knez Z. Modelling high pressure extraction processes. *Comput Chem Eng.* 2001;25:879-886.
16. Goodarznia I, Eikani MH. Supercritical carbon dioxide extraction of essential oils: Modeling and simulation. *Chem Eng Sci.* 1998;53:1387-1395.
17. Puiggene J, Larrayoz MA, Recasens F. Free liquid-to-supercritical fluid mass transfer in packed beds. *Chem Eng Sci.* 1997;52:195-212.
18. Bothun GD, Knutson BL, Strobel HJ, Nokes SE, Brignole EA, Diaz S. Compressed solvents for the extraction of fermentation products within a hollow fiber membrane contactor. *J Supercrit Fluids.* 2003;25:119-134.
19. Gros HP, Bottini S, Brignole EA. A group contribution equation of state for associating mixtures. *Fluid Phase Equilib.* 1996;116:537-544.

20. Gros HP, Bottini SB, Brignole EA. High pressure phase equilibrium modeling of mixtures containing associating compounds and gases. *Fluid Phase Equilib.* 1997;139:75-87.
21. Perry RH, Green DW. *Perry's Chemical Engineers' Handbook*. New York, NY: McGraw-Hill; 1998.
22. Bueno JL, Suarez JJ, Medina I. Experimental binary diffusion coefficients of benzene and derivatives in supercritical carbon dioxide and their comparison with the values from the classical correlations. *Chem Eng Sci.* 2001;56:4309-4319.
23. Pierre FX, Souchon I, Athes Dutour V, Marin M. Membrane-based solvent extraction of sulfur aroma compounds: Influence of operating conditions on mass transfer coefficients in a hollow fiber membrane contactor. *Desalination.* 2002;148:199-204.
24. Bothun GD, Knutson BL, Strobel HJ, Nokes SE. Mass transfer in hollow fiber membrane contactor extraction using compressed solvents. *J Membr Sci.* 2003;227:183-196.

Appendix

Table A1. Comparison between Experiments and Our Model for Extraction of Ethanol with Subcritical Propane

S/F	Q_w (mL/min)	Eff	Experimental Efficiency*	Calculated Efficiency in the Literature*
1	0.15	5.2	6.8	6.5
	0.25	4.7	6.4	6.5
	0.5	3.7	9.0	6.5
	0.75	3.1	11.3	6.4
	1.0	2.6	9.2	6.2
	1.5	2.0	13.1	5.8
	2.0	1.7	11.0	5.2
2	0.15	8.7	7.6	13.0
	0.25	7.3	10.4	13.0
	1.0	3.3	9.5	10.3
	1.5	2.4	13.1	8.6
	2.0	1.9	9.9	12.0
3	0.15	11.3	4.7	19.5
	0.25	9.0	10.4	19.1
	1.0	3.6	14.0	12.7
	1.5	2.5	13.4	9.9
	2.0	2.0	14.3	8.2
10	0.1	23.7	9.7	56.3

*Data from Bothun et al.[18]

Table A2. Comparison between Experiments and Our Model for Extraction of Acetone with Subcritical Propane

S/F	Q_w (mL/min)	Eff	Experimental Efficiency*	Calculated Efficiency in the Literature*
1	0.15	79.84	38.9	99.2
	0.25	74.24	36.6	95.9
	0.5	59.2	21.8	84.8
	1.0	39.7	22.6	66.8
2	0.5	72.2	30.4	90.8
	1.0	45.1	22.1	72.3
3	0.15	>100	64.6	100.0
	0.25	>100	63.9	99.3
	0.5	77.9	33.5	92.4
	1.0	47.3	23.9	74.0
10	0.1	>100	90.6	100.0

*Data from Bothun et al.[18]

Table A3. Comparison between Experiments and Our Model for Extraction of Ethanol with Subcritical Carbon Dioxide

S/F	Q_w (mL/min)	Eff	Experimental Efficiency*	Calculated Efficiency in the Literature*
3	0.15	24.6	15.2	29.4
	0.25	23.7	10.4	27.5
	0.5	21.1	4.7	22.0
	1.0	17.0	9.9	15.1
10	0.1	60.3	31.9	69.5

*Data from Bothun et al.[18]

Table A4. Comparison between Experiments and Our Model for Extraction of Acetone with Subcritical Carbon Dioxide

S/F	Q_w (mL/min)	Eff	Experimental Efficiency*	Calculated Efficiency in the Literature*
3	0.15	100.0	96.1	100.0
	0.25	100.0	89.6	100.0
	0.5	100.0	68.9	100.0
	1.0	94.1	67.9	95.1

*Data from Bothun et al.[18]

Manuscript received Mar. 12, 2004, and revision received July 26, 2004.